Applied Ocean Research 154 (2025) 104366

Contents lists available at ScienceDirect

Applied Ocean Research

journal homepage: www.elsevier.com/locate/apor

Research paper

Mechanical performance after service of hybrid synthetic mooring lines for weather buoys

Peter Davies [a,*], Nicolas Lacotte [a], Gaspard Fourestier [b], Iroise Petton [b]

[a] IFREMER Centre Bretagne, Research and Technology Development Unit, 29280 Plouzané, France
[b] GEPS Techno, 1 Rte de la Croix Moriau, 44350 Guérande, France

ARTICLE INFO

Keywords:
Mooring
Synthetic
Strength loss
Abrasion

ABSTRACT

Synthetic fibre ropes are increasingly popular for mooring lines of marine structures. The adoption of polyester ropes for deep water offshore platforms has resulted in a large material database, but the development of floating wind turbines has widened the scope to include more dynamic loadings and more compliant mooring lines are being developed. These are needed both for the turbines, particularly in shallow water, but also for the weather buoys which are used to obtain data on site conditions before wind park installation. This study has investigated the residual properties of weather buoy mooring lines based on hybrid fibres, polyester with polyolefin fibres. A set of lines was recovered from two shallow water sites after up to 2.5 years at sea. Significant loss of strength was measured after service, up to 50%. The reasons for this, mainly damage to external polyester fibres caused by mussel attachment, are discussed.

1. Introduction

Synthetic fibre mooring lines are widely used to maintain floating structures in position. Considerable experience has been gathered from the use of polyester ropes for station-keeping of floating deepwater oil and gas platforms (Del Vecchio, 1992; De Pellegrin, 1999; Bugg et al., 2004; Rossi et al., 2010), and there is growing interest in polyamide fibre ropes for floating offshore wind turbines in shallow water (Weller et al., 2015; Banfield and Ridge, 2017; Pham et al., 2019; Sørum et al., 2023). Another important application is the station-keeping of moored, instrumented buoys. These include weather buoys, which may be 1 to 10 meters in diameter and are exposed to very harsh ocean conditions. They are used to provide wave and wind data to evaluate future offshore wind park installations. The mooring lines must hold the buoy in position while absorbing considerable amounts of energy from wind, wave and current loading. One option for this application which has been employed for several years is a hybrid polyester/polyolefin rope. The combination of the excellent durability of polyester and the low density polyolefin fibres such as polypropylene appears very attractive and some data have been published on the properties of such ropes (Khalid et al., 2020). Stiffnesses were shown to be intermediate between polyester and polyamide. However, very few data are available on the in-service degradation of these materials. Polyester ropes have received most attention. Gage et al described tests performed on a large diameter polyester fibre rope recovered after 10 years in service in the Gulf of Mexico (Gage et al., 2021). The residual strengths of subropes were actually higher, by up to 20%, than the initial measured break strength after manufacture. This was explained by fibre reorientation under load in service. Beltran & Williamson proposed both analyticakl (Beltrán and Williamson, 2009) and numerical models (Beltrán and Williamson, 2011) of the influence of damage in jacketed polyester ropes.

Lian et al also discussed residual strength of polyester ropes (Lian et al., 2022). They distinguished different types of damage due to the following factors: (1) rope handling during installation; (2) wear experienced during service; (3) ingress of sand and marine growth; (4) material and manufacturing defects; and (5) local sub-rope or element rupture during service. By introducing damage through knife cuts they established an empirical residual strength model. Ayers et al discussed degradation of polyester mooring lines in contact with sediment. Early experience offshore had shown that damage caused by particle ingress could significantly reduce rope strength (by up to 30% in less than a year), and subsequently the inclusion of sand filters between cover and cores became common practice (Ayers et al., 2013).

Flory discussed tests to determine residual strength of different rope materials and concluded that strength loss could be directly correlated with damaged area for polyester and nylon but that HMPE ropes were

* Corresponding author.
E-mail address: peter.davies@ifremer.fr (P. Davies).

https://doi.org/10.1016/j.apor.2024.104366
Received 20 April 2024; Received in revised form 29 October 2024; Accepted 2 December 2024
Available online 12 December 2024

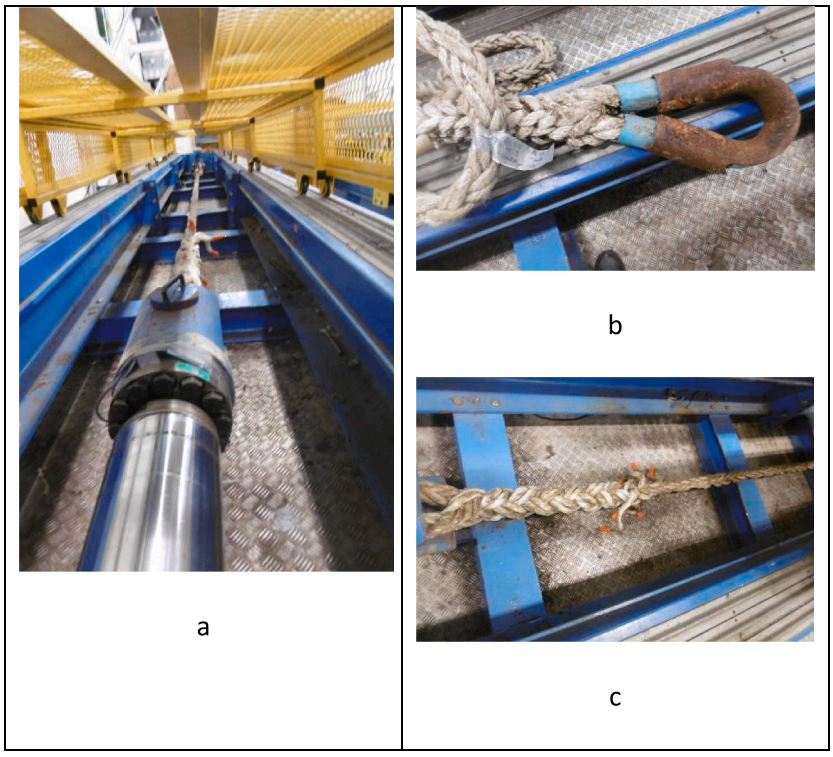

Fig. 1. a) Rope sample on test frame, 1000 kN capacity, 10 meters long b) Original termination, steel thimble, c) New termination, spliced loop.

much more sensitive to damage (Flory, 2008). Again yarn cutting was used to simulate service damage. McCorkle et al performed a study on forty HMPE tug lines after up to 2 years in service (McCorkle et al., 2003). They showed that the residual strengths were generally high. However, the loading conditions of towing lines (drum compression, shock loads) are quite different from those encountered by mooring lines.

Most of the previous scientific studies were based on artificial damage and in-service rope experience tends to be discussed at trade conferences rather than in scientific papers. To the authors' knowledge no previous publications have provided strength data on hybrid ropes after service. It is therefore difficult to quantify their durability in such applications and to assess whether they may be re-used. This is the aim of the study reported here. Samples were recovered after service at two sites and tests were performed to determine residual tensile properties.

First, the materials and service conditions will be described. Then the residual rope properties will be presented. And finally reasons for strength loss will be discussed.

2. Materials and test methods

The mooring lines tested here are 44 mm diameter hybrid Polyester (PET)/Polyolefin ropes with a nominal minimum break load of 493 kN. Each rope yarn is made of polyester multifilaments twisted around polyolefin inner monofilaments, roughly 50% of each by weight. The ropes tested are marketed under the *Euroflex*™ brand name, designed for

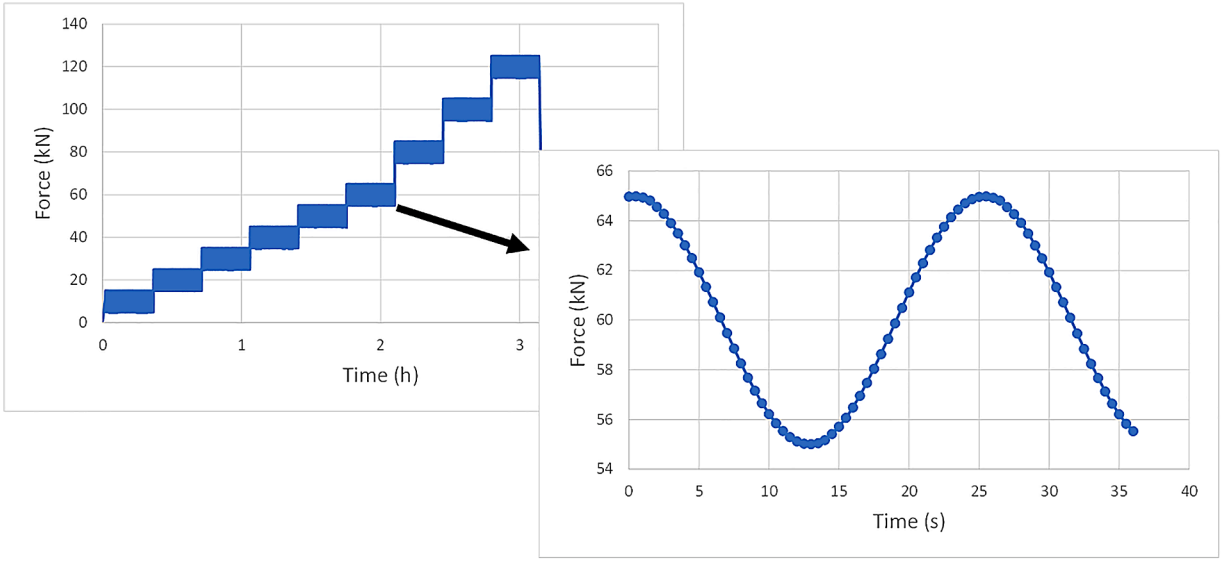

Fig. 2. Loading cycle sequence for stiffness tests. Detail shows measured data points for cycling at 60 ± 5 kN.

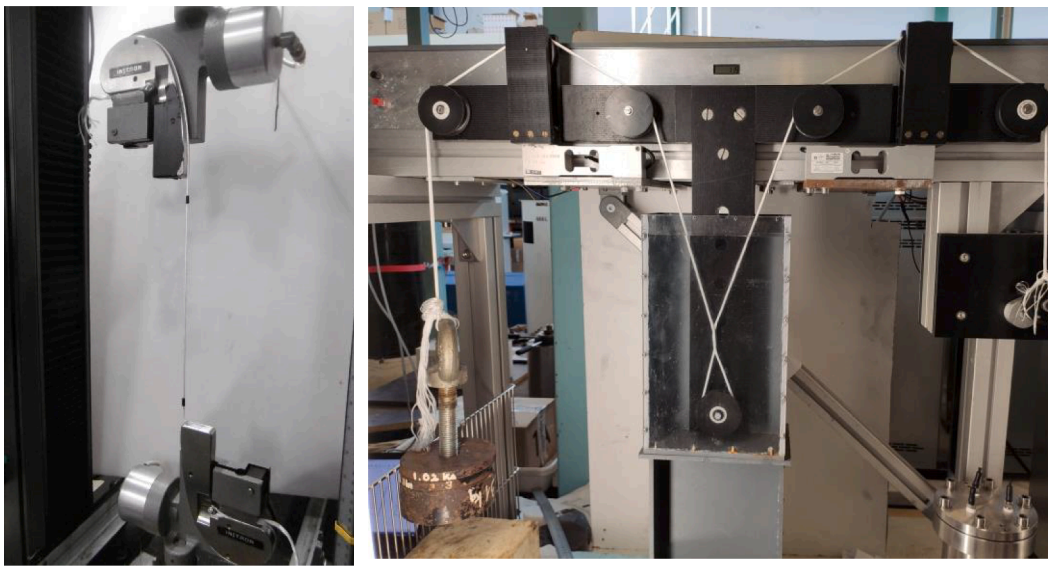

(a) (b)

Fig. 3. Rope yarn tests. a) Tension loading with pneumatic grips, two digital cameras to measure strain in the free length between grips. b) Rope yarn on Rope yarn abrasion test set-up.

mooring and towing for shipping and offshore operations (lankhorstropes.com/synthetic-fibre-ropes/euroflex), although other ropemakers have similar hybrid fibre products.

Sixteen full scale ropes were tested in tension to break on a 1000 kN test frame (annual load cell calibration by an external company) at the IFREMER Centre in Brest, Fig. 1a. All were performed dry, under servo-hydraulic load control at a loading rate of 10% of nominal break load per minute. The test bench is 10 meters long. In most cases, in order to fit the sample on the test frame one original termination, a loop around a steel thimble with a protective sheet, Fig. 1b, was retained and a new splice of similar length, Fig. 1c was made at the other end. For the original terminations, a protective sheet was placed between the rope and the thimble. This resulted in an overall sample length around 6 meters.

Stiffness measurements were made on some samples. For these a wire transducer was fixed to the central rope section between splices over a length of around 2 meters. The load sequence was as shown below, Fig. 2; 50 cycles at 9 different mean loads (10, 20, 30, 40, 50, 60, 80, 100 and 120 kN) with an amplitude of 5 kN and a cycling period of 25 s. The dynamic stiffness, KrD, was determined from the slope of a linear regression of load-strain datapoints for the last 5 cycles at each mean load, normalized by the nominal break load (493 kN).

Additional mechanical tests were performed on rope yarns extracted from the ropes, in tension, Fig. 3a, and in abrasion, (rope yarn on rope yarn) Fig. 3b. The former were performed dry on a 10 kN Instron™ 5596 test frame under displacement control at 50 mm/minute in a temperature (21 ± 1 °C) and humidity (50 ± 5%) controlled laboratory. In total 110 tensile tests were performed, 52 on internal rope yarns and 58 on external. The abrasion tests used an up-sized yarn-on-yarn test frame based on the ASTM standard 6611 (ASTM D6611-16, 2016) with 230 mm between the upper pulleys and the lower pulley 325 mm below a line between the two upper pulleys. The diameter of the pulleys was 50 mm. A single loading weight was used; 4.28 kg. More details on the test machine are available elsewhere (Bain et al., 2023), the cycling rate was 1 Hz. The abrasion tests were performed fully immersed in natural sea water with 1.5 turns applied to twist the rope yarns together in the abrasion zone. In total 27 samples were tested, three for each condition.

Additional calorimetry (DSC) analyses were made to examine polymer microstructure, on TA DSC25 equipment, with a ramp at 10 °C/minute from −50 to 300 °C. This provides information on melting enthalpies of the fibres, which could indicate changes in the degree of crystallinity between new and used samples. Three samples were analyzed for each condition. Optical and scanning electron microscopy were used to investigate damage in ropes. For the latter an FEI Quanta 200 microscope was used with an Au-Pd coating to avoid charging.

The 13 used lines came from two sites, in the Irish Sea and next to Oleron Island, off the French Atlantic coast. They were employed on weather buoys for different periods (less than 30 months in all cases).

Table 1
Samples tested.

Sample	History	Comments
New 1	Storage inside	Stiffness measurements
New 2	Storage Inside	Stiffness measurements
New 3 UV	Storage outside 6 months	Stiffness measurements
Oleron 1	27 months	
Oleron 2	27 months	Stiffness measurements
Oleron 3	27 months	
Irish Sea		
1	10 months	Stiffness measurements
2	10 months	Stiffness measurements
3	23 months. Lower	Stiffness measurements
4	9 +6 months	
5	23 months. Upper	
6	23 months	Stiffness measurements
7	9 +6 months. Upper	Cut strands beneath thimble
8	9 +6 months. Lower	Tested with floats in place
9	23 months	Badly corroded thimble
10	9 +6 months	Tested with floats in place

N.B. '9+6' corresponds to 9 months service then 6 months disconnected on the seafloor before recovery.

Table 2
Extreme site conditions with a return period of one year.

	Irish sea	Oleron
Moored depth (m)	11 - 20	>30
Extreme wind speed, (m/s)	21.36	17.71
Extreme current speed (m/s)	1.21	0.46
Extreme wave height Hs (m)	7.14	6.86
Buoy Depth variation (m), tidal range + storms	6.24	10.64

Table 3
Name and period of the databases used to perform the extreme value analysis.

	Irish Sea		Oleron	
	Name of database	Period of database	Name of database	Period of database
Wind Database	CFS	1979–2019	France-WRF9k	1991–2015
Current and sea level Database	ATLNE2000	2006–2015	AQUI250	2006–2015
Wave Database	Copernicus-north-sea-waves	1980–2022	HOMERE	1994–2012

Table 1 describes all the samples.

There is a clear difference in the environments at the two sites, with Irish Sea conditions significantly more severe than Oleron. This was confirmed by an analysis of site data providing extreme conditions over a one-year period (Table 2).

These values are constructed from extreme values analyses, performed on data extracted from various numerical databases (Caires, 2011). These databases are presented in Table 3 below.

The CFS3D wind database is based on the global hourly Climate Forecast System produced by the NCEP (National Center for Environmental Prediction) (Saha et al., 2010; Saha et al., 2014). The wind database France-WRF9k was built by VORTEX using the computer code Weather Research and Forecasting (WRF) over the French west and north coasts. The HOMERE database was developed by Ifremer using the numerical wave model WaveWatchIII® (WW3) version 4.09 (Boudière et al., 2013). The Copernicus-north-sea-waves is a database derived from a WaveWatchIII® (WW3; version 4.18) numerical wave model, with a 1.5 km grid centered on the United Kingdom at 3-hourly sample interval (Graham et al., 2018). ATLNE2000 and AQUI250 databases are 2D,

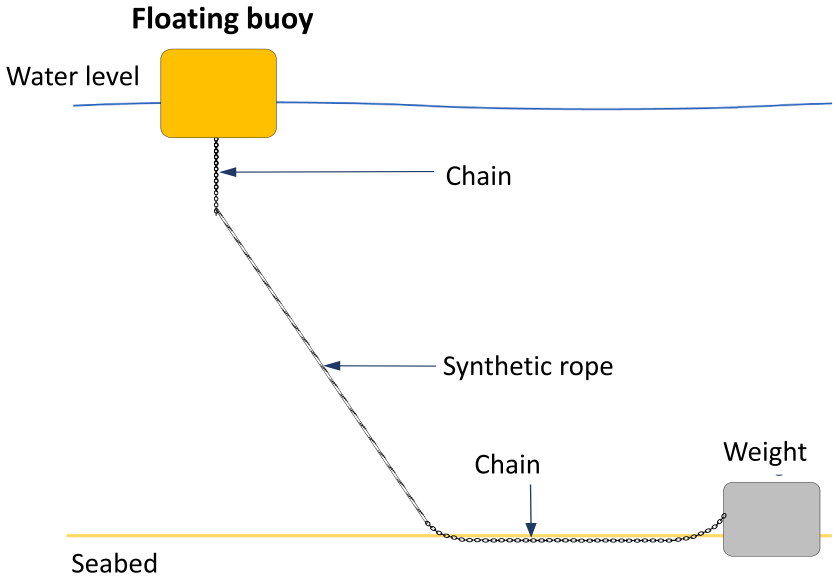

Fig. 4. Buoy design.

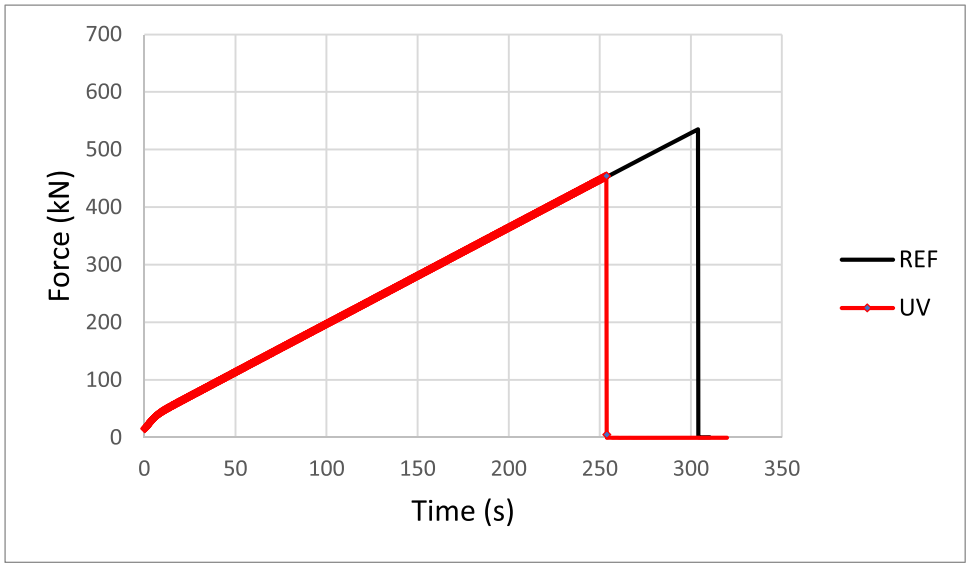

Fig. 5. Force versus time plots, new ropes.

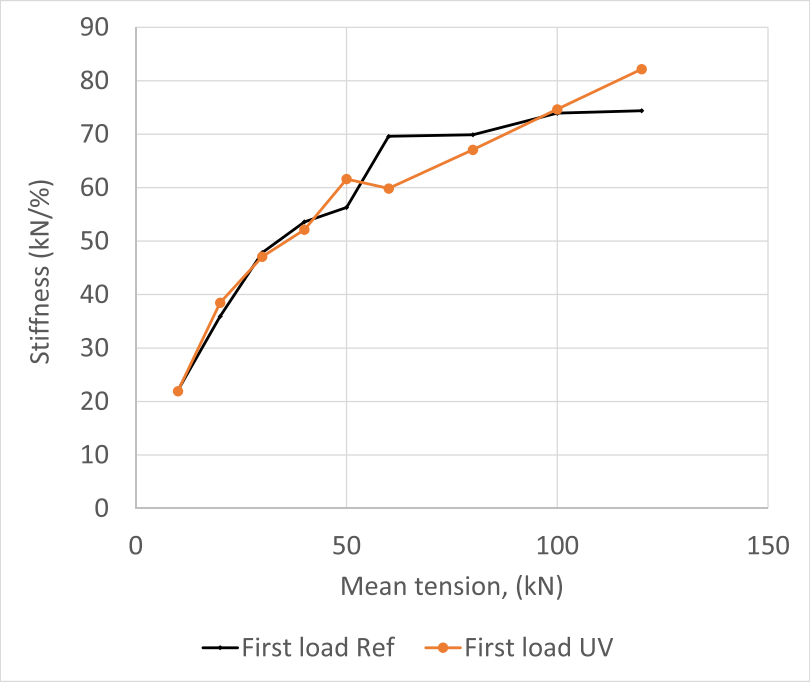

Fig. 6. Stiffness values, new and UV aged ropes, first loading.

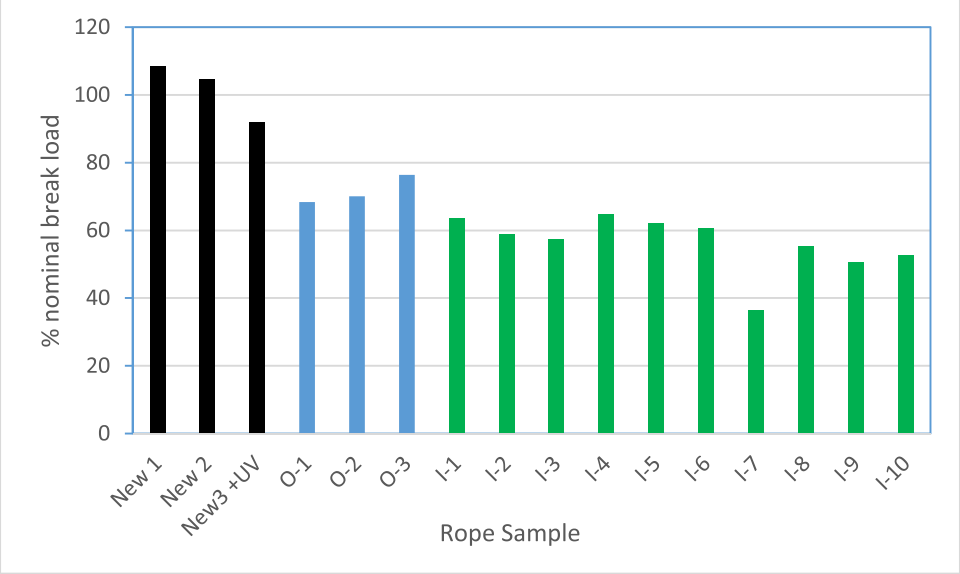

Fig. 7. Summary of break loads as a percentage of nominal break load (493 kN) O : Oleron. I : Irish Sea.

depth-averaged numerical simulations, performed by Ifremer using the numerical hydrodynamical model MARS2D (Model for Applications at Regional Scale, (Lazure and Dumas, 2008)).

The 13 used lines come from weather buoy moorings with similar design (Fig. 4). In total four weather buoys were moored with these lines: three in the Irish Sea and one off the Oleron coast. The mooring lines are made up of, from top to bottom, a few meters of chain, then the Euroflex™ rope and chains followed by a weight. The length of bottom chain and weight are chosen to guarantee that the weather buoy stays in position. The Euroflex™ rope is present in the water column, a few meters below the water level and a few meters above the seabed. The 13 used lines are sections of the rope part present in these moorings.

3. Results

First, three unused rope samples were tested. Two had been stored inside while the third had been stored outside, exposed to sunlight for 6 months. Dynamic stiffness measurements were made, at loads up to 125 kN (25% nominal break load), Fig. 2, then the samples were loaded to failure. Fig. 5 shows the load-displacement plots for the three break tests. The new samples failed at similar loads, 516 and 535 kN, above the manufacturer's nominal value of 493 kN, while the break load for the sample stored outside for 6 months was around 8% lower at 454 kN. This shows the importance of protecting ropes during storage, particularly when they do not have an external cover.

A comparison between the stiffnesses measured on new and UV aged ropes (first loading, no bedding-in) is shown in Fig. 6. The values are

Fig. 8. Failure zones, a) at end of splice, example I-2, b) damaged strand due to thimble, sample I- 7, one of three severed strands, c) broken steel thimble, I-9.

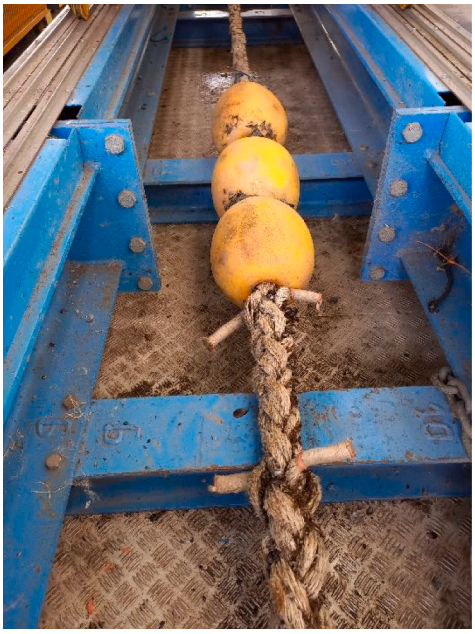

Fig. 9. Test with floats.

very similar, within experimental scatter, and there is a significant influence of mean load on KrD values. This mean load effect, a higher stiffness at higher mean loads, has been shown previously for polyester ropes (François and Davies, 2008).

Fig. 7 shows all the break loads for the used ropes, plotted as a percentage of the nominal break load value (taken as 493 kN).

It is apparent that all the recovered samples have lost tensile strength during service. The majority of the used samples failed at the end of the splices, Fig. 8a; this was the case for the three Oleron samples and the first six Irish sea ropes. The two lowest break loads, for Irish sea samples 7 and 9, correspond to termination damage related to the steel thimbles, Fig. 8b and c respectively.

In the first case there appears to have been extensive wear between the end of the thimble and the rope; the blue protective sheath was no longer in place, and three of the eight strands were completely severed (Fig. 7b). In the second case the thimble was badly corroded and cracked after 23 months at sea, Fig. 7c, resulting in rope failure at the back of the eye.

Two samples were tested with floats on the lines, (used to avoid seafloor contact), Fig. 9, in order to examine whether this affected the rope behaviour. These were Irish sea ropes 8 and 10. The break loads were lower than for the ropes which failed at the end of the splice. Fig. 10 shows the failure zones, which are at the interface between the rope and the end of the floats in the free length between the splices. These floats were held in place by small diameter cords and those may be responsible for the premature ruptures. This will be discussed further below.

Finally, Fig. 11 shows examples of stiffness measurements made on used ropes. The values are quite close to those measured on the new ropes. These and other measurements suggest that over these service lives the rope stiffness for these loading conditions remains very close to the values for new ropes.

4. Discussion

The results presented in the previous section indicate very significant losses in the strengths of these mooring lines after less than 3 years in service (Fig. 6). The average strength for the Irish Sea ropes which failed at the end of the splices and not in the original terminations is around 300 kN (40% reduction). The Oleron average is around 350 kN (30%

Fig. 10. Failure zones of ropes tested with floats.

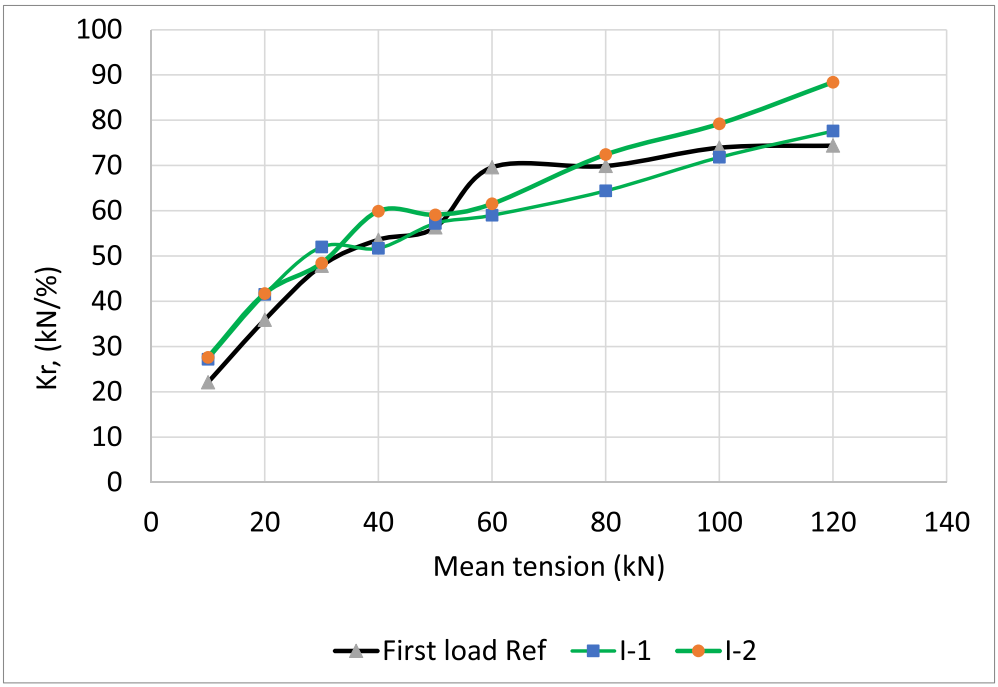

Fig. 11. Example of stiffness test results during first loading after service.

Table 4
Characteristic temperatures and melt enthalpies, PET fibres from exterior of strands.

Sample	Peak melt temperatures°C	Melt Enthalpy, J/g	Estimated mean PET crystallinity, %
New	257, 257, 257	51.1, 45.6, 51.5	36.3
Oleron	258, 260, 259	47.0, 53.0, 51.7	37.2
Irish Sea	258, 258, 258	51.9, 49.1, 49.4	36.9

loss). There could be various reasons for these drops:

- Changes in fibre microstructure causing embrittlement.
- Changes in the interactions between fibres (coating).
- Damage development due to high loads in service.
- Surface damage initiating premature failure.

All these possibilities are discussed below. The first, changes in fibre microstructure, was checked even though extensive experience with polyester in the offshore oil and gas industry suggests that it is unlikely to explain such large strength losses unless there is a particular problem with fibre quality. The characteristic melting temperatures of the fibre materials were analysed by calorimetry (DSC) on new samples and after service. Table 4 shows the results for PET samples removed from the exterior of strands. A mean value for degree of crystallinity of the PET

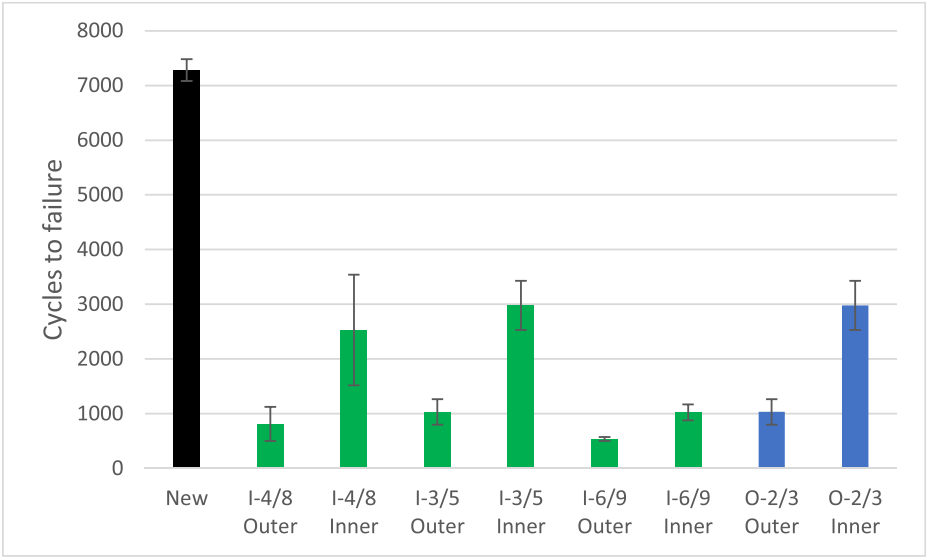

Fig. 12. Summary of abrasion tests, performed on rope yarns taken from exterior and interior of strands.

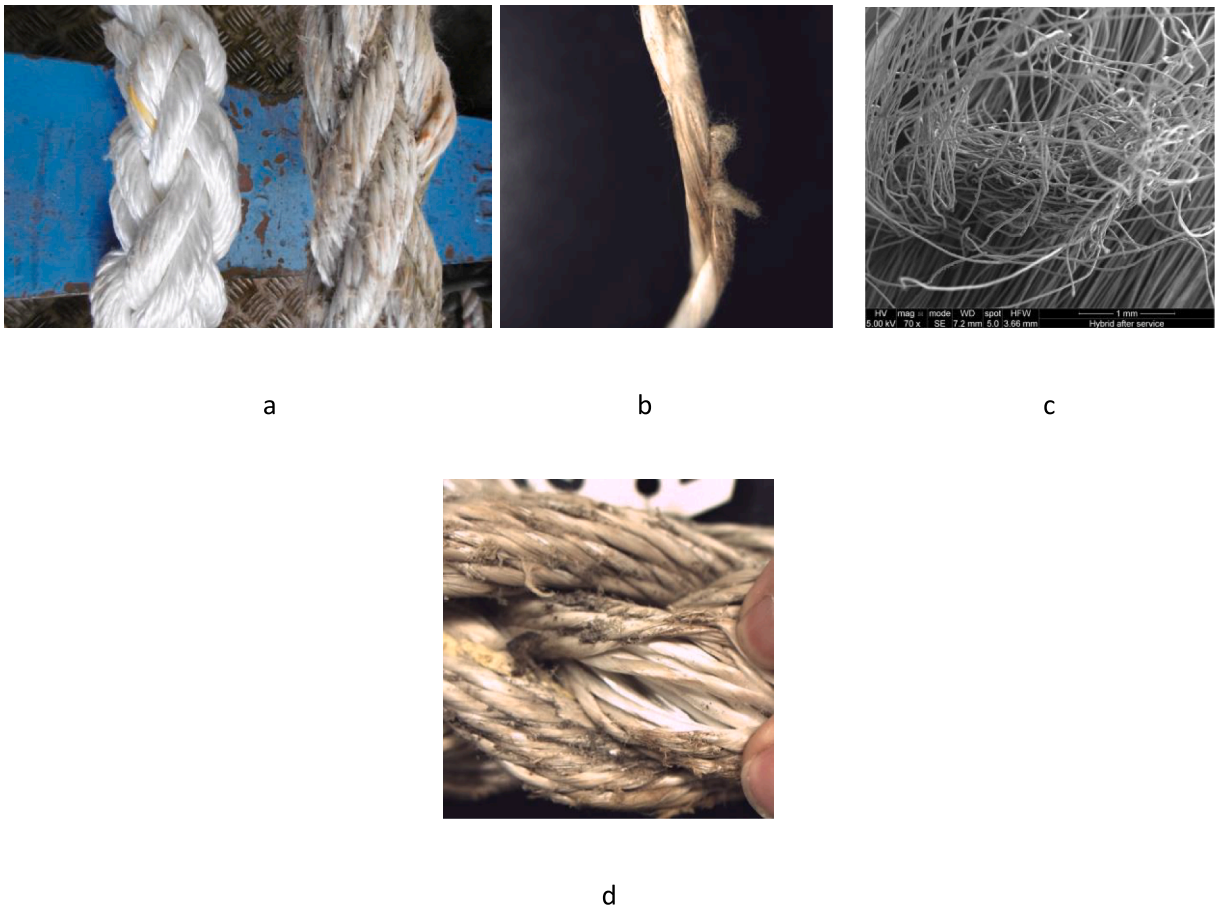

Fig. 13. a) New and aged (cleaned) ropes, b) aged rope yarn with defect, c) SEM image of damaged surface fibres, d) rope yarns in strand separated to reveal clean inner rope yarns.

fibres is shown, based on a value of 136 J/g for 100% crystallinity (Starkweather et al., 1983; Kong and Hay, 2003).

The DSC results indicated that the constituent fibres were indeed those announced (PET, PE and PP) and that there is not a significant change in fibre crystallinity after service. While this does not exclude changes to microstructure it suggests that this is unlikely to be a major factor in property changes.

Second, fibres used in marine applications generally have a specific coating, a marine finish, which protects them during service. External and internal rope yarns were removed from ropes and their rope yarn-

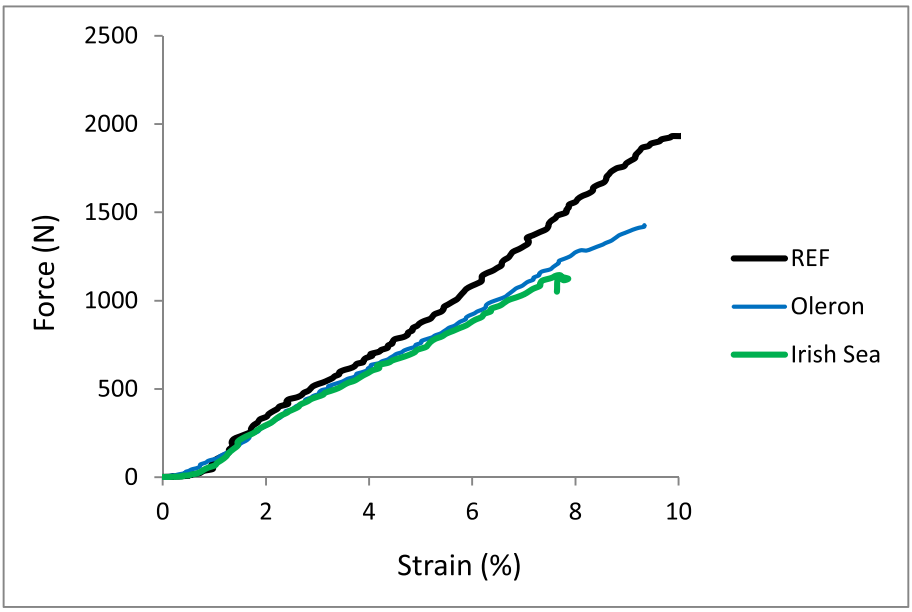

Fig. 14. Examples of load-strain plots, tensile tests on new and aged external rope yarn samples.

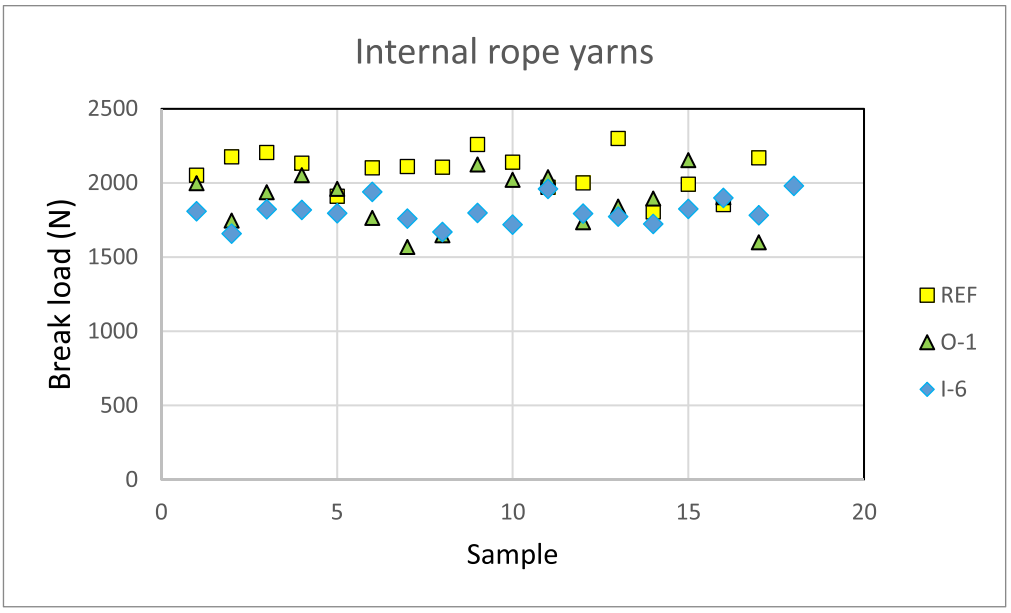

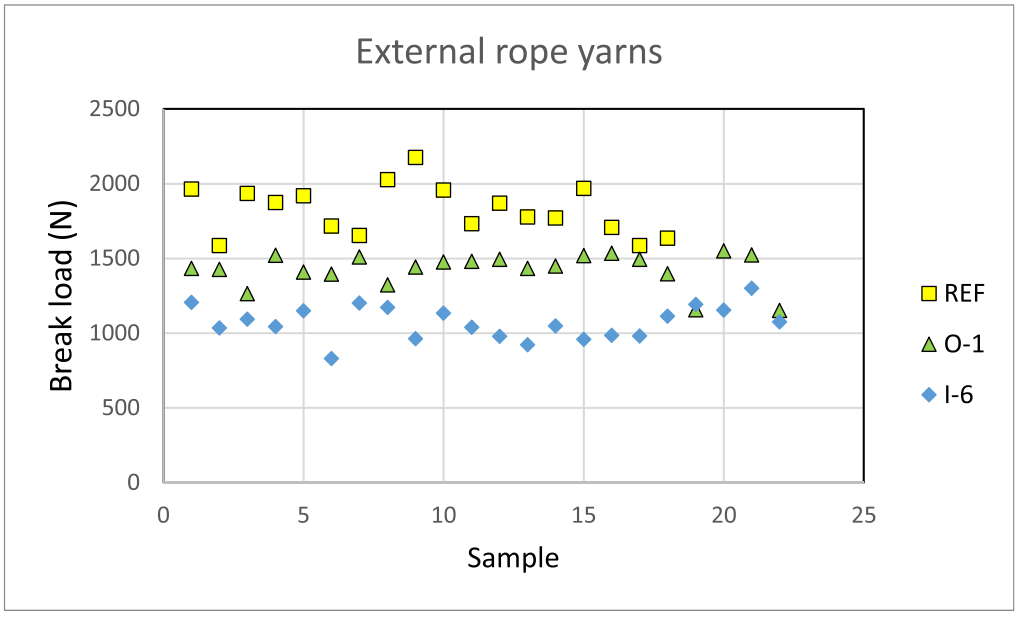

Fig. 15. Tensile test results, inner and outer rope yarns from New, Oleron-1 and Irish Sea-6 strands

on-rope yarn abrasion performance was examined, both before and after service. Given the rope yarn construction (polyolefin fibres covered by PET) this is a test of abrasion between PET fibres. Fig. 12 summarizes the results.

N.B. The rope yarn samples used for the abrasion tests presented above were taken from short (one-meter) sections removed from the full scale mooring lines. The numbering system indicates their position with respect to the rope numbers in Table 1 and Fig. 7. For example, the samples named I-3/5 is taken from the Irish Sea rope between rope test samples I-3 and I-5.

These results clearly show a very significant drop in abrasion resistance for the external rope yarns. It is also interesting to note a lesser but significant drop for the internal rope yarns of the recovered samples, this may be related to removal of surface finish, as visually the inner yarns appear much smoother and less damaged than the external yarns. The very large drop in outer surface abrasion resistance suggests that it is surface damage which is responsible for strength loss. Fig. 13 shows details of the rope surface at different scales.

In order to investigate where the strength loss comes from, individual rope yarn samples were extracted and tested in tension. If the fibres have been overloaded, resulting in damage, then one would expect both outer and inner fibres to be affected. Rope yarns were therefore removed from the outer and inner regions of one new and two aged (Oleron-1 and Irish sea-6) rope strands and loaded to failure. At least 15 samples were tested for each.

Fig. 14 shows examples of typical load-strain results for the different tensile tests, Fig. 15 summarizes the tensile test results. The initial stiffnesses are similar for all conditions but loads and strains to failure drop after service.

Failure was seen to initiate at fibre damage regions, such as the one shown in Fig. 13b. Several defects such as these can be seen along each external rope yarn sample from the Irish Sea, but there are very few on internal rope yarns.

It is clear from analysis of these results that there is a significant drop

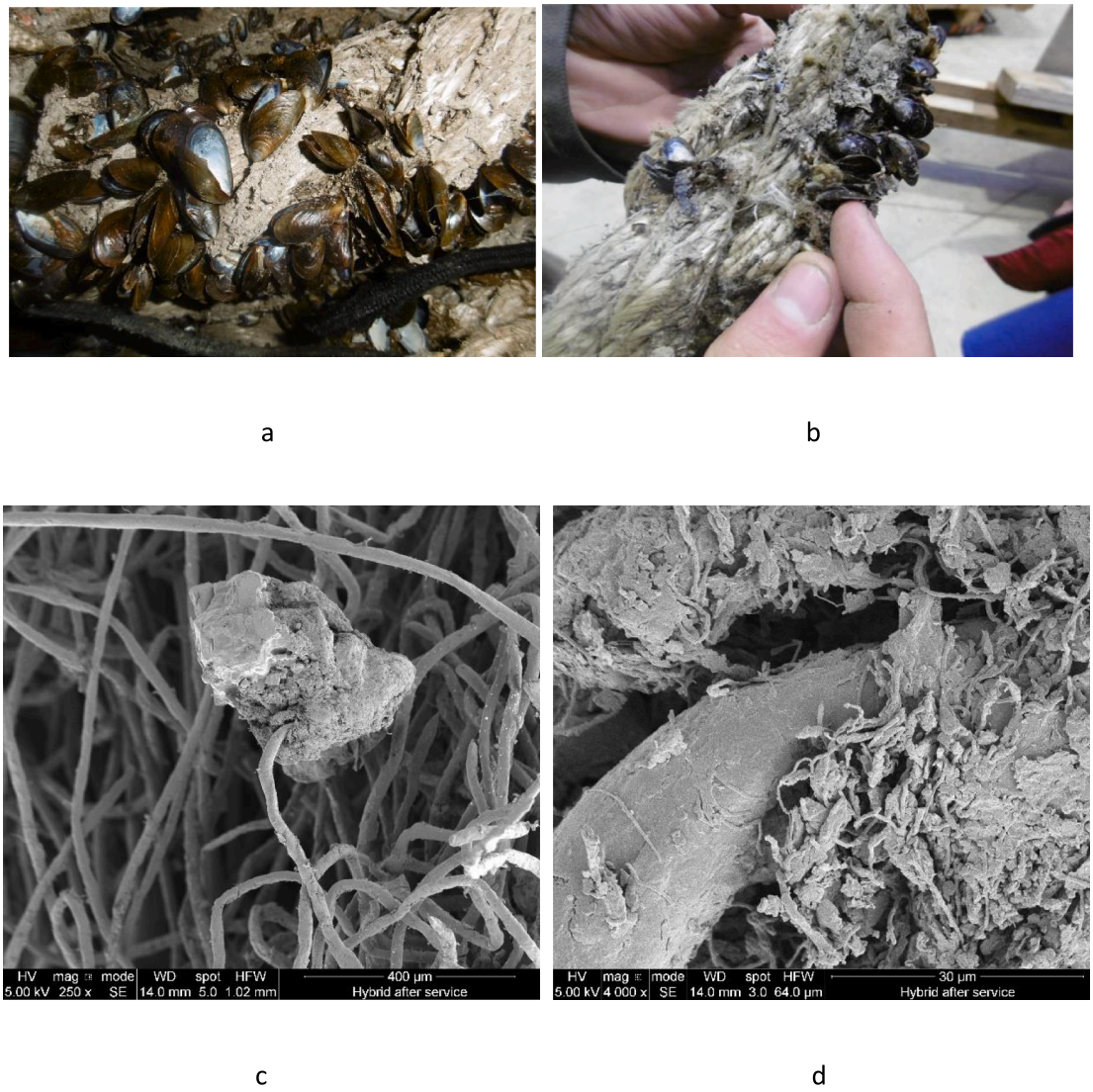

Fig. 16. Upper: Mussels fixed on mooring line before cleaning (strand diameter 18 mm) Lower: SEM images of damaged, bonded fibres on rope surface.

Fig. 17. Thimble contact causing damage to strands after protective cover failure (I-7) or corroded thimble failing during test (I-9).

in external rope yarn break loads for the Irish Sea samples, on average around 50%. New mean outer and inner rope yarn strengths are 1826 N and 2075 N with coefficients of variation (CV) of 7 and 9%. The corresponding values for aged rope yarns are 1072 N (CV 10%) and 1806 N (CV 5%) for the Irish sea and 1427 (CV 8%) and 1880 N (CV 10%) for Oleron. For both sites the mean strengths of inner yarns are similar, around 90% of the reference strength. However, the outer yarn strengths of Oleron samples are much closer to the original new values (around 80% compared to 60% for the Irish Sea). To a first approximation, based on 22 outer rope yarns in a strand and 18 inner yarns, a purely additive use of these values would indicate residual strengths of 84 and 72 % for these two ropes. Measured residual values, with respect to the mean measured new rope strength (taken as 525 kN), were lower, 64% for Oleron and 54% for the Irish sea. This may reflect the braided rope geometry and the degradation in the interfaces between elements shown by the rope yarn-on-rope yarn results. A more realistic rope model would be needed to include these effects. Such a model was used in previous work on hybrid ropes (Khalid et al., 2020), and by using degraded rope yarn properties as input data could help to optimize mooring design.

These results underline the loss in strength of external fibres, with more severe loss for Irish Sea ropes. This may be due to more severe environmental conditions but those would also affect internal fibres. A more likely explanation appears to be the more widespread surface fouling of the Irish Sea lines (shallower moored depths, Table 2), which caused more extensive surface fibre damage, resulting in the abrasion and tensile performance changes described above.

Examples of the state of mooring lines after recovery before cleaning are shown in Fig. 16. These buoys are moored in shallow water and there is considerable marine growth attached, particularly mussels (Fig. 16a, b). While many of these drop off during transport and handling some remain, and these were usually removed manually or with high pressure water cleaning. An examination of the removal of mussels revealed that some are strongly bonded and hard to remove without damage to fibres. Mussels adhere to surfaces by secreting 'byssus' fibres which act as anchor lines, with adhesive plates as the anchors. Their adhesion properties have been extensively studied (Brown, 1952; Crisp et al., 1985; Waite, 1987; Bell and Gosline, 1966; Waite and Harrington, 2022). If this adhesive anchor can surround fibres on the rope surface, in a similar way to rope-grown mussel farming, it will indeed be very difficult to remove them without damaging the rope. Fig. 16c and d show SEM images of an area where PET fibres appear to be bonded to the biological adhesive deposited by the mussel. We suggest that the reduction in rope strength is primarily caused by macro-fouling causing multiple damage initiation sites.

In addition to the change in rope behaviour due to surface damage, the test results also highlight two additional causes of premature failure which can result in even larger strength losses. The first is the influence of the thimble at the termination. Fig. 17 shows the importance of protecting the rope from the steel thimble. In this case the impregnated fabric interface has been severely damaged on the right hand side so the rope could rub against the steel, which led to the sectioning of strands such as the one shown previously in Fig. 8b.

The second aggravating factor is the presence of floats. This is another important issue, as floats are required for many marine applications and here they are used to keep the lower part of the line off the sea bed. In order to maintain them at the required depth they are attached to the anchor line with small diameter cords, Fig. 10. These restrict local movement of the strands and can produce a stress concentration. The break loads recorded for the two tests with floats were around 10 and 14% lower than the mean of those without (I-1 to I-6). This is a relatively small difference, but the fact that in both cases failure was observed close to the floats suggests that this may be a problem in applications where longer durability is needed. While there have been some modelling studies on submerged buoys (Palm and Eskilsson, 2020) more work is needed to quantify their influence on fibre rope behaviour.

5. Conclusions

Samples of mooring lines from weather buoys have been tested after service to examine their residual properties. These lines are employed in very severe environments, subjected to storms, high winds and strong currents. The results from two sites, Oleron and the Irish Sea, reveal significant strength losses of 30 and 40% respectively. These have been analysed and can be attributed to damage in external polyester fibres. This is mainly associated with mussel attachment which disturbs external fibres and creates local stress concentrations. The effect of these is clearly apparent in rope yarn tests.

In particular cases even higher strength losses were measured, due to termination damage. The presence of floats also affects the failure location.

These results are important as they both quantify potential strength losses, which are quite uniform for each site, and highlight the care needed with key design features which can lead to higher strength losses (thimbles and floats). These should be taken into account in mooring line design. An external coating would help to reduce the influence of marine fouling and protect load-bearing fibre cores, and could enable these mooring lines to be re-used. This is being examined in ongoing work.

CRediT authorship contribution statement

Peter Davies: Writing – review & editing, Writing – original draft, Project administration, Methodology, Investigation, Conceptualization. **Nicolas Lacotte:** Writing – review & editing, Visualization, Investigation. **Gaspard Fourestier:** Writing – review & editing, Validation, Resources, Investigation. **Iroise Petton:** Writing – review & editing, Validation, Methodology, Investigation.

Declaration of competing interest

The authors declare that they have no known competing financial interests or personal relationships that could have appeared to influence the work reported in this paper.

Funding

This research did not receive any specific grant from funding agencies in the public, commercial, or not-for-profit sectors.

Acknowledgements

The authors are grateful to Nicolas Gayet and Arnaud Le Moan of IFREMER for the SEM observations, abrasion tests and calorimetry measurements.

References

ASTM D6611-16, Standard Test Method for Wet and Dry Yarn-on-Yarn Abrasion Resistance (2016).

Ayers RR, Del Vecchio CJ, Devlin PV, Head W, Effects of fiber rope – seabed contact on subsequent rope integrity, 2013, OTC 24047-MS.

Bain, C, Davies, P, Riou, L, Marco, Y, Bles, G, Damblans, G, 2023. Experimental evaluation of the main parameters influencing friction between polyamide fibers and influence of friction on the abrasion resistance. J. Text. Inst. 114 (7), 998–1006. https://doi.org/10.1080/00405000.2022.2105075.

Banfield, S, Ridge, IM, 2017. Fatigue durability of nylon rope for permanent mooring design. In: OCEANS 2017-Aberdeen. IEEE, pp. 1–9. https://doi.org/10.1109/OCEANSE.2017.8084825.

Bell, EC, Gosline, JM, 1966. Mechancal design of mussel byssus: material yield enhances attachment strength. J. Exper. Biol. 199, 1005–1017.

Beltrán, JF, Williamson, EB, 2009. Investigation of the damage-dependent response of mooring ropes. J. Eng. Mech.-ASCE 135, 1237–1247.

Beltrán, JF, Williamson, EB, 2011. Numerical procedure for the analysis of damaged polyester ropes. Eng. Struct. 33 (5), 1698–1709.

Boudière, E, Maisondieu, C, Ardhuin, F, Accensi, M, PineauGuillou, L, Lepesqueur, J, 2013. A suitable metocean hindcast database for the design of Marine energy converters. Int. J. Mar. Energy 34 (2013), e40–e52.
Brown, CH, 1952. Some structural proteins of *Mytilus edulis*. Q. J. Microsc. Sci. 93 (4), 487–502.
Bugg, DL, Vickers, DT, Dorchak, CJ, 2004. Mad Dog project: Regulatory approval process for the new technology of synthetic (polyester) moorings in the Gulf of Mexico. In: Proceedings of the Offshore Technology Conference. Houston, TX, USA, 3–6 May.
Caires, S, 2011. Extreme Value Analysis: Wave Data. WMO. JCOMM Technical Report No. 57.
Crisp, DJ, Walker, G, Young, GA, Yule, AB, 1985. Adhesion and substrate choice in Mussels and Barnacles. J Colloid and Interface science 104 (1), 40–50.
Del Vecchio, C.J.M., 1992. Light Weight Materials for Deep Water Moorings. University of Reading, Reading, UK. PhD Thesis.
De Pellegrin, I., 1999. Manmade fiber ropes in deepwater mooring applications. In: Proceedings of the Offshore Technology Conference. Houston, TX, USA, 3–6 May.
Flory, J, 2008. Assessing strength loss of abraded and damaged fiber rope. In: OCEANS 2008 - MTS/IEEE Kobe Techno-Ocean. Kobe, Japan, pp. 1–12. https://doi.org/10.1109/OCEANSKOBE.2008.4531103.
François, M, Davies, P., 2008. Characterization of polyester mooring lines. In: Proceedings of the ASME 2008 27th International Conference on Offshore Mechanics and Arctic Engineering (OMAE)Estoril, Portugal. ASME, pp. 169–177. https://doi.org/10.1115/OMAE2008-57136. June 15–20.
Gage, CR, Liagre, PF, Heyl, CN, Del Vecchio, C, 2021. Dropped polyester mooring line qualification for reuse. In: Offshore Technology Conference.
Graham, JA, O'Dea, E, Holt, J, Polton, J, Hewitt, HT, Furner, R, Guihou, K, Brereton, A, Arnold, A, Wakelin, S, Castillo Sanchez, JM, Mayorga Adame, CG, 2018. AMM15: a new highresolution NEMO configuration for operational simulation of the European northwest shelf. Geosci. Model Dev. 11, 681696.
Khalid, F, Davies, P, Halswell, P, Lacotte, N, Thies, PR, Johanning, L, 2020. Evaluating mooring line test procedures through the application of a round robin test approach. J. Mar. Sci. Eng. 8, 436. https://doi.org/10.3390/jmse8060436.
Kong, Y, Hay, JN, 2003. The enthalpy of fusion and degree of crystallinity of polymers as measured by DSC. Eur. Polym. J. 39 (8), 1721–1727.
lankhorstropes.com/synthetic-fibre-ropes/euroflex.
Lazure, P, Dumas, F, 2008. An externalinternal mode coupling for a 3D hydrodynamical model for applications at regional scale (MARS). Adv. Water Res. 31 (2), 233–250.
Lian, Y, Zhang, B, Zheng, J, Liu, H, Ma, G, Yim, SC, Zhao, Y, 2022. An upper and lower bound method for evaluating residual strengths of polyester mooring ropes with artificial damage. Ocean Eng. 262. https://doi.org/10.1016/j.oceaneng.2022.112243.
McCorkle, E, Chou, R, Stenvers, D, Smeets, P, Vlasblom, M, Grootendorst, E, 2003. Fatigue and residual strength of fiber tuglines. In: OCEANS 2003. San Diego, CA, USA, 2, pp. 1058–1063. https://doi.org/10.1109/OCEANS.2003.178487.
Palm, J, Eskilsson, C, 2020. Mooring systems with submerged buoys: influence of buoy geometry and modelling fidelity. Appl. Ocean Res. 102, 102302.
Pham, H.D., Cartraud, P., Schoefs, F., Soulard, T., Berhault, C., 2019. Dynamic modeling of nylon mooring lines for a floating wind turbine. Appl. Ocean Res. 87, 1–8.
Rossi, R, Del Vecchio, CJM, Ricardo, CFG, 2010. Fiber moorings, recent experiences and research: moorings with polyester ropes in petrobras: experience and the evolution of life cycle management. In: Paper presented at the Offshore Technology Conference. Houston, Texas, USA. https://doi.org/10.4043/20845-MS. May 2010.
Saha, S, et al., 2010. The NCEP climate forecast system reanalysis. Bull. Am. Meteorol. Soc. 91, 1015–1057.
Saha, S, Moorthi, S, Wu, X, Wang, J, Nadiga, S, Tripp, P, Behringer, D, Hou, YT, Chuang, HY, Iredell, M, Ek, M, Meng, J, Yang, R, Mendez, MP, Hvd, Dool, Zhang, Q, Wang, W, Chen, M, Becker, E, 2014. The NCEP climate forecast system version 2. J. Clim. 27, 2185–2208. https://doi.org/10.1175/JCLI-D-12-00823.1.
Sørum, SH, Fonseca, N, Kent, M, Faria, RP, 2023. Assessment of nylon versus polyester ropes for mooring of floating wind turbines. Ocean Eng. 278, 114339. https://doi.org/10.1016/j.oceaneng.2023.114339.
Starkweather, HW, Zoller, P, Jones, GA, 1983. The heat of fusion of poly(ethylene terephthalate). J. Polym. Sci. Polym. Phys. Ed. 21 (2), 295–299.
Waite, JH, 1987. Nature's underwater adhesive specialist. Int. J. Adhes. Adhes. 7 (1), 9–14.
Waite, JH, Harrington, MJ, 2022. Following the thread: Mytilus mussel byssus as an inspired multi-functional biomaterial. Can. J. Chem. 100 (3). https://doi.org/10.1139/cjc-2021-0191.
Weller, SD, Johanning, L, Davies, P, Banfield, SJ, 2015. Synthetic mooring ropes for marine renewable energy applications. Renew. Energy 83, 1268–1278.